Self-Assembled Structures

DOI: 10.1002/anie.200806267

A Supramolecular Hydrogen-Bonded Network as a Diffusion Barrier for Metal Adatoms**

*Christophe Silien, Minna T. Räisänen, and Manfred Buck**

The versatility and precision afforded by molecular structures make surface-based supramolecular self-assembly a promising strategy for addressing the lower end of the nanoscale.[1,2] Whereas precisely defined patterns can be straightforwardly generated, subsequent modification, such as functionalization, secondary patterning, or macroscopic interfacing, is required for such structures to become useful. One critical issue is thus the compatibility of supramolecular structures with further modification steps. Moreover, mechanisms determining processes on a larger scale are not expected to apply at the length scale of supramolecular structures because the reduced dimensionality alters the kinetics of processes and changes the influence of energy-determining factors. From these two points, it is evident that the development of self-assembled nanostructures requires the establishment of routes towards higher levels of complexity and understanding of the underlying mechanisms.

First steps along the aforementioned directions have been taken by demonstrating that porous supramolecular structures can be used as templates to control arrangement of other molecules, such as C_{60},[3–5] coronene,[6] or porphyrins.[4] Following this scheme, a hybrid structure, combining a network with self-assembled monolayers (SAMs), was demonstrated recently.[7] A supramolecular hydrogen-bonded network composed of PTCDI and melamine was first formed on a Au(111) surface and thiols, such as ω-(4′-methylbiphenyl-4-yl)ethanethiol (BP2), were adsorbed into its pores (Figure 1). As SAMs allow very flexible tailoring of interfaces,[8,9] such network/SAM hybrid structures potentially allow versatile and precise chemistry at the nanoscale and thus warrant further exploration. Given the opportunities afforded by potential-controlled processing, our interest lies in metal electrodeposition and herein we focus on the underpotential deposition (UPD) of copper. UPD involves deposition of one to two monolayer(s) of a metal onto a foreign metal substrate and occurs positive of the Nernst potential.[10] Beside the fact that it precedes bulk deposition, it also enables modification of SAMs by intercalation at the SAM–substrate interface, which alters the thiol–substrate bond and thus enhances SAM stability. This effect can be exploited for the generation of composed SAMs.[11] However, for the generation of precisely defined nanometer-sized patterns, exact control of the deposition is required. As shown recently,[12] the challenge lies in the substantial lateral diffusion of Cu adatoms at the SAM–substrate interface, as it limits resolution. If, however, the supramolecular network acted as barrier for adatom diffusion, the precisely defined dimensions of the network/SAM hybrid structure combined with metal UPD would bear significant potential for nanoscale patterning (Figure 1b). Yet, it is unclear how Cu adatoms, which are another order of magnitude smaller than the molecular building blocks, affect the network structure with its relatively weak noncovalent bonds. Hence, it is important to elucidate the mutual influence of hybrid structure and metal UPD.

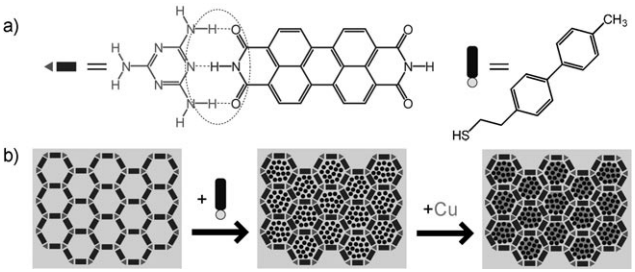

Figure 1. a) Triple hydrogen bonding motif of 1,3,5-triazine-2,4,6-triamine (melamine) and perylene-3,4,9,10-tetracarboxylic diimide (PTCDI), and structure of ω-(4′-methylbiphenyl-4-yl)ethanethiol (BP2). b) Scheme for the solution-based generation of a hybrid structure starting from the hexagonal porous PTCDI–melamine hydrogen-bonded network. The filling of the pores by SAM molecules is followed by electrochemical UPD of Cu.

In this work, BP2 was chosen as the thiol molecule to allow for a comparison with uniform BP2 SAMs, for which the properties[13] and mechanism of Cu UPD[12] have been studied in detail. The scanning tunneling microscope (STM) image of a network/BP2 hybrid structure after Cu UPD (Figure 2a), clearly demonstrates that, as in the case of adamantanethiol,[7] the hexagonal arrangement of the BP2 cells is maintained upon Cu deposition. The stability of the pattern is also evidenced by the distinct bright spots in the corresponding fast Fourier transform (FFT; Figure 2a, inset). Furthermore, the whole surface is affected equally, which suggests that Cu UPD is complete and uniform, in pronounced contrast to Cu UPD on uniform BP2 SAMs (Figure 2b). Referring to our previous work for details,[12] we summarize herein the major features of UPD on uniform BP2 SAMs. The growth reveals itself as circular patches originating at defects and expanding radially. Cu forms a

[*] Dr. C. Silien, Dr. M. T. Räisänen, Dr. M. Buck
EaStCHEM School of Chemistry, University of St Andrews
North Haugh (UK)
Fax: (+44) 1334-463-808
E-mail: mb45@st-and.ac.uk
cjcs@st-and.ac.uk
Homepage: http://ch-www.st-andrews.ac.uk/eastchem/profiles/sta/buck.html

[**] This work was supported by the UK Engineering and Physical Science Research Council (EPSRC).

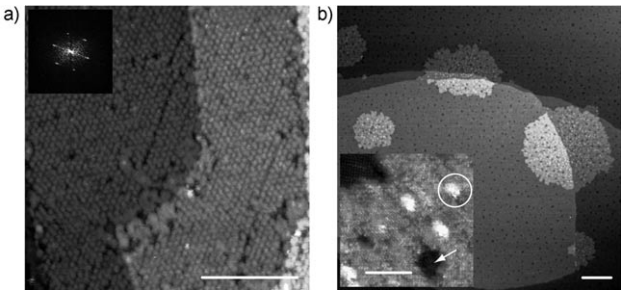

Figure 2. a) STM image of a network/BP2 hybrid structure on Au(111) after Cu UPD (1 min at 100 mV). Fast Fourier transform shown in inset. b) STM images of a uniform BP2 SAM after partial Cu UPD (1 h at 100 mV). A vacancy island and a nanoisland are marked by an arrow and a circle, respectively. Vacancy islands are also visible as small dark spots in the main image. Scale bars are 50 nm for main images and 5 nm for inset.

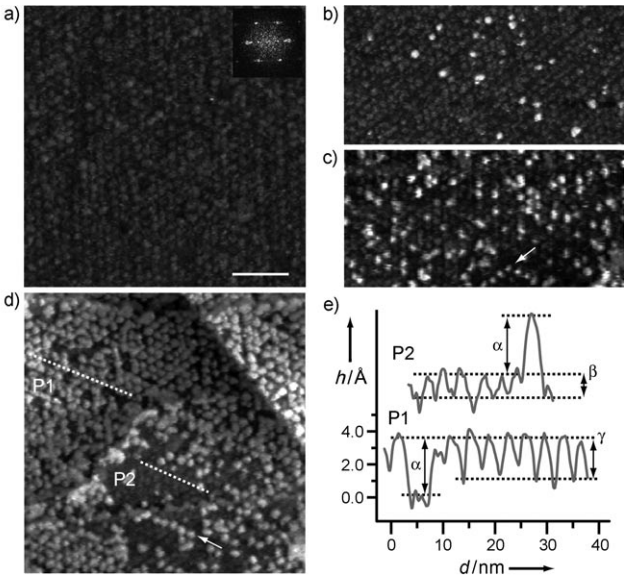

Figure 3. STM images of the evolution of Cu UPD on a network/SAM hybrid structure on Au(111). Starting from the native structure (a), UPD is accomplished in steps with progressive reduction of the potential and with a deposition time of 1 min for each step. b) 200 mV, c) 160 mV, d) 140 mV. e) Height profiles P1 and P2 extracted from the image shown in (d). Scale bar is 20 nm. All STM images are shown at the same scale.

continuous film at the SAM-Au interface, i.e., underneath the BP2 molecules, which is reflected by a measured height difference of approximately 2.5 Å between modified and native SAM areas. Additional nanoislands form randomly on patches as seen more clearly in the inset. Their emergence is presumed to reflect accommodation of interfacial stress.[12] Comparing uniform SAMs with network/BP2 hybrids reveals fundamental differences in several points. First, vacancy islands, i.e., monoatomic deep depressions in the substrate, are absent in the hybrid structure while clearly discernible as dark spots in Figure 2b[14,15] on the uniform BP2 SAM. Second, no nanoislands emerge upon Cu UPD on the network/BP2 structure. Indeed, only buried Cu patches reproducing the network symmetry and periodicity are seen in Figure 2a. Both observations can be rationalized by the variation in the amount of stress generated: for uniform SAMs, it can easily exceed a critical value, thus, causing restructuring of the SAM/Au interface, while for hybrid structures, it should be reduced owing to fragmentation of the SAM into small compartments. SAM formation and SAM–substrate interfacial structure are therefore pronouncedly different for hybrid structures and uniform SAMs. In the presence of the network, Cu UPD is also greatly accelerated, highlighting further differences. For hybrid structures, it is accomplished within a few minutes whereas, at comparable potentials, only a fraction of the surface is modified after hours in the case of uniform BP2 SAMs.

However, not only the Cu deposition rate is affected by the network but changes in the UPD mechanism are also seen. These can be inferred from snapshots of the evolution of Cu UPD on a network/BP2 sample (Figure 3). To allow monitoring of its early stages, the deposition was started at a rather positive potential (200 mV), in which case it proceeds rather slowly. The potential was then altered in steps towards more cathodic values. Starting from the native network/BP2 hybrid structure (Figure 3a), Cu UPD led to the random emergence of protrusions with lateral dimensions defined by the pores of the supramolecular network (Figure 3b). At this stage, the density of Cu UPD sites was also significantly higher than the density of Cu patches on uniform SAMs (Figure 2b). After the second deposition step (Figure 3c), isolated protrusions continued to appear. UPD in cells adjacent to those already modified was occasionally detected, but occurred in a statistical, uncorrelated way, that is, systematic radial spreading of UPD modification does not occur in this case, in stark contrast to uniform SAMs. After the third step, most cells had been modified by Cu (Figure 3d), even though small areas where most cells were not modified were still seen. Thus, a few isolated protrusions remained but the inverse case, where nonmodified cells were surrounded by modified ones, was significantly more frequent. Both cases are detailed by the height profiles P1 and P2 (extracted from Figure 3d and shown in Figure 3e). P1 runs across adjacent cells, of which all but one are Cu-modified, whereas for P2 the situation is reversed. Continuation of the deposition ultimately results in all cells being modified (Figure 2a). P1 and P2 reveal that the increase in apparent height of the cells on network/BP2 hybrid structures following Cu UPD was approximately 3.5 Å (α), whereas, on uniform SAMs, a height increase of roughly 2.5 Å was measured.[12] Given that these height variations depend sensitively on details in the SAM structure and bonding to the substrate, they again highlight pronounced differences between the two systems either before or after UPD, or at both stages. In combination with the absence of both vacancy islands and nanoislands, it can be concluded that the two states are different, in particular with respect to the amount of stress accumulated, as stated above.

The height profiles (Figure 3e) revealed a larger corrugation along Cu-modified cells (ca. 2.7 Å, γ, P1) in comparison to nonmodified ones (ca. 1.6 Å, β, P2). Whereas absolute values depend to some extent on STM tip geometry and tunneling conditions, relative values can be directly compared

when extracted from the same STM image. This increase in corrugation upon Cu UPD is consistent with the interpretation that Cu was only deposited in the pores and not in areas of the network molecules, as depicted in Figure 1b. Although this result does not represent a definitive proof, as it is unclear how tunneling conditions vary for thiols and network molecules upon Cu deposition, compelling evidence came from the way Cu UPD evolves during the stepwise deposition, which also reveals that the network acts as a diffusion barrier for Cu adatoms. These conclusions were derived, firstly, from the presence of single Cu-modified and of single nonmodified cells (surrounded by Cu-modified ones) that were isolated over significant periods of time and, secondly, from the absence of a systematic radial progression of the filling of neighboring cells, which would have been indicative of an extensive interfacial diffusion of the Cu adatoms, as in the case of uniform SAMs.[12] Chain-like modifications of adjacent pores (as marked by arrows in Figure 3c,d) are occasionally detected. Even though it is reasonable to assume that such modifications are related to structural imperfections in the network/BP2 hybrid structure, the detailed mechanism is not clear at present. Distortions of the structure could either enable copper to diffuse to neighboring pores or facilitate UPD into specific cells, owing to, for example, variations in molecular packing in SAM islands.

The model for Cu UPD on a network/SAM modified Au(111) electrode is illustrated in Figure 4, together with the contrasting mechanism for a uniform SAM. For the latter, growth of Cu UPD proceeds exclusively by lateral diffusion at the SAM–substrate interface with metal adatoms being only reduced at defects which are not intrinsic to the SAM, leading to a rather slow deposition.[12] In contrast, for network/SAM hybrid structures, the supramolecular network represents a significant disruption in the SAM continuity and greatly facilitates the approach of Cu^{2+} ions to the Au substrate and, thus, their reductive deposition. Cu UPD nucleation is therefore possible at each pore, resulting in a more uniform and faster intercalation of Cu across the surface. Variation in the rate at which this occurs (see coexistence of modified and native areas in Figure 3d) can be explained by differences in the structural perfection of the SAM islands, with the number of molecules adsorbed in a network pore varying by up to three, as inferred from molecularly resolved experiments using adamantanethiol.[7] Accordingly, the activation barrier for intercalation of Cu varies. The other decisive effect of the network is, as discussed above, that lateral interfacial diffusion is suppressed between adjacent cells, i.e., Cu adatoms are confined within the pore where they have been reduced. We note at this point that, beyond our general interest in thiols for chemical modification of interfaces, a thiol-filled network was chosen as it reduces the rate of UPD compared to an empty one, and thus allows monitoring of the temporal evolution of Cu deposition. Furthermore, high resolution imaging is facilitated by thiols protecting Cu against oxidation. Whether the barrier properties of the network are exactly the same with the SAM absent is unclear at present. Nonetheless, since Cu UPD does not require SAMs,[10] there are no obvious reasons why the mechanism should not apply to empty networks as well.

In summary, Cu UPD on a SAM templated by a hydrogen-bonded network differed markedly from a uniform layer, which was reflected by the absence of vacancy islands and nanoislands on the network/SAM system, and by the different height changes upon Cu intercalation, which, in turn, revealed that the SAM structures and/or SAM–substrate interfaces were different. Of most interest regarding applications was the role of the supramolecular network as a diffusion barrier. Suppression of lateral diffusion between adjacent cells, that is, confinement of Cu adatoms on a scale below 3.5 nm, and, at the same time, much faster and better controllable UPD renders network/SAM hybrid systems of potential use for precise modification at the nanoscale, which, if controlled down to a single pore, would open up unprecedented possibilities.

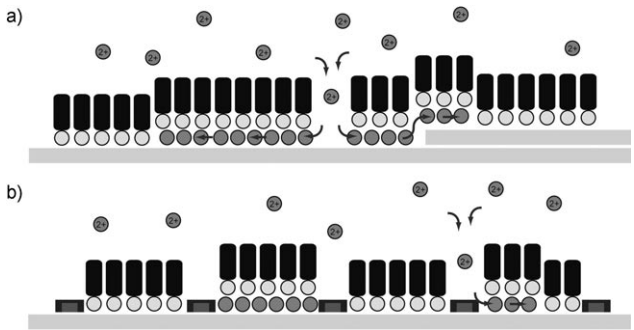

Figure 4. Illustrations of Cu UPD on (a) a uniform BP2 SAM and (b) a network/BP2 hybrid structure. On the uniform SAM, growth originates from an isolated defect and proceeds through lateral interfacial diffusion.

Experimental Section

N,*N*-Dimethylformamide (DMF) solutions of PTCDI–melamine were prepared from saturated solutions of PTCDI (ca. 98%; Alfa Aesar) and melamine (99.9%; Sigma–Aldrich), diluted 1:25 and 1:4, respectively, in DMF. Substrates (Au/mica; 300 nm gold; Georg Albert PVD) were flame-annealed before immersion in the PTCDI/melamine solution for network formation (1 min at 373 K). BP2 (for synthesis, see ref. [16]) was self-assembled into the network pores from DMF solution (ca. 100 μM) in 5–10 min. The samples were rinsed with absolute ethanol and blown dry after these two steps. Cu UPD was achieved in a Teflon electrochemical cell using aqueous electrolytes of $CuSO_4$ (5 mM)/H_2SO_4 (0.5 μM) for network/BP2 and $CuSO_4$ (5 mM)/H_2SO_4 (50 mM) for uniform BP2 layers, with Cu and Pt wires as reference and counter electrodes, respectively. The samples were rinsed with deionized H_2O and ethanol, and blown dry with N_2 prior to measurements in air. STM images were recorded with a PicoScan (Molecular Imaging) and tips shaped by mechanically cutting a Pt/Ir (80:20) wire (0.25 mm diameter). Bias and currents were typically 250–500 mV (tip positive) and 1.5–5 pA.

Received: December 22, 2008
Revised: February 6, 2009
Published online: April 3, 2009

Keywords: electrochemistry · self-assembly · monolayers · supramolecular chemistry · surface chemistry

[1] J. V. Barth, *Annu. Rev. Phys. Chem.* **2007**, *58*, 375 – 407.
[2] S. De Feyter, F. C. De Schryver, *Chem. Soc. Rev.* **2003**, *32*, 139 – 150.
[3] J. A. Theobald, N. S. Oxtoby, M. A. Phillips, N. R. Champness, P. H. Beton, *Nature* **2003**, *424*, 1029 – 1031.
[4] M. Stöhr, M. Wahl, H. Spillmann, L. H. Gade, T. A. Jung, *Small* **2007**, *3*, 1336 – 1340.
[5] D. Bonifazi, A. Kiebele, M. Stohr, F. Y. Cheng, T. Jung, F. Diederich, H. Spillmann, *Adv. Funct. Mater.* **2007**, *17*, 1051 – 1062.
[6] M. Blunt, X. Lin, M. D. Gimenez-Lopez, M. Schroder, N. R. Champness, P. H. Beton, *Chem. Commun.* **2008**, 2304 – 2306.
[7] R. Madueno, M. T. Räisänen, C. Silien, M. Buck, *Nature* **2008**, *454*, 618 – 621.
[8] J. C. Love, L. A. Estroff, J. K. Kriebel, R. G. Nuzzo, G. M. Whitesides, *Chem. Rev.* **2005**, *105*, 1103 – 1170.
[9] F. Schreiber, *J. Phys. Condens. Matter* **2004**, *16*, R881 – R900.
[10] M. A. Schneeweiss, D. M. Kolb, *Phys. Status Solidi A* **1999**, *173*, 51 – 71.
[11] D. Oyamatsu, H. Kanemoto, S. Kuwabata, H. Yoneyama, *J. Electroanal. Chem.* **2001**, *497*, 97 – 105.
[12] C. Silien, M. Buck, *J. Phys. Chem. C* **2008**, *112*, 3881 – 3890.
[13] P. Cyganik, M. Buck, T. Strunskus, A. Shaporenko, G. Witte, M. Zharnikov, C. Wöll, *J. Phys. Chem. C* **2007**, *111*, 16909 – 16919.
[14] C. A. McDermott, M. T. McDermott, J. B. Green, M. D. Porter, *J. Phys. Chem.* **1995**, *99*, 13257 – 13267.
[15] K. Edinger, A. Gölzhäuser, K. Demota, C. Wöll, M. Grunze, *Langmuir* **1993**, *9*, 4 – 8.
[16] H. T. Rong, S. Frey, Y. J. Yang, M. Zharnikov, M. Buck, M. Wühn, C. Wöll, G. Helmchen, *Langmuir* **2001**, *17*, 1582 – 1593.

